

Supporting Information

Self-assembly-integrated tumor targeting and electron transfer programming towards boosting tumor type I photodynamic therapy

Wenlong Chen^{a, b ‡}, Zehui Wang^{b ‡}, Gaobo Hong^b, Jianjun Du^b, Fengling Song*^{a, b}

and Xiaojun Peng^b

^a Shenzhen Research Institute of Shandong University, A301 Virtual University Park in South District of Shenzhen, 518057, P.R. China.

^b State Key Laboratory of Fine Chemicals, Frontiers Science Center for Smart Materials Oriented Chemical Engineering, Dalian University of Technology, Dalian 116024, P. R. China.

[‡] Wenlong Chen and Zehui Wang contributed equally in this work.

* Correspondence author. Email: songfl@sdu.edu.cn, songfl@dlut.edu.cn.

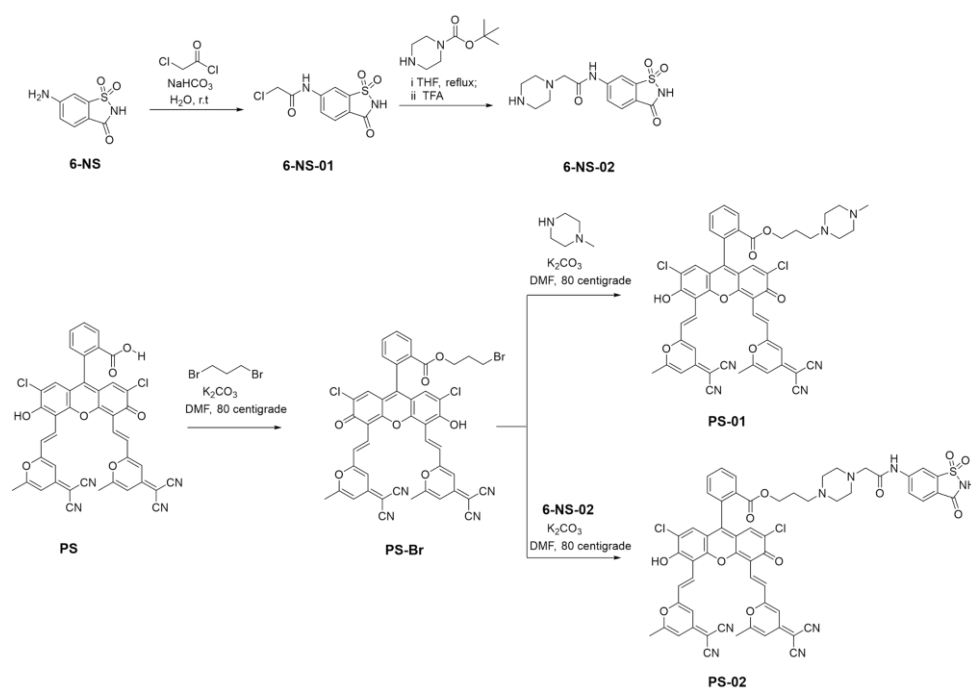
1. MATERIALS AND INSTRUMENTS INTRODUCTIONS.

All reagents acquired were used directly without further processing if not stated. chloroacetyl chloride, anhydrous 1-boc-piperazine, 6-aminosaccharin, 1,3-dibromopropane, and N-methyl piperazine were purchased from Energy Chemical in Shanghai of China. Dihydrorhodamine 123 (DHR 123), commercial membrane dye DiO, 2',7'-dichlorodihydrofluorescein diacetate (DCFH-DA), Calcein-AM/PI double stain kit and acridine orange were purchased from Nanjing Keygen Biotech Co., Ltd.

3-(4,5-dimethylthiazol-2-yl)-2,5-diphenyl-2h-tetrazoliubromide (MTT) was purchased from Sigma-Aldrich. UV-Vis absorption spectra were performed on a Cary 60 UV-Vis spectrophotometer from Agilent Technologies. Fluorescence emission spectra were performed on Cary Eclipse from Agilent Technologies. Tumor cells fluorescence imaging were obtained on a confocal laser scanning microscope (CLSM) from Olympus LS (FV1000). Small animals' fluorescence imaging was carried out on NightOWL II LB983 from BIRTHOLD.

2. EXPERIMENTS.

2.1 General Procedure of Synthesizing PS-01 and PS-02.



Scheme S1 Schematic diagram of the synthetic route of the molecules **PS-01** and **PS-02**.

Synthesis of ligand **6-NS-02**

6-NS-01 was synthesized by the amidation reaction between **6-NS** and chloroacetyl chloride¹. **6-NS-01**, Yield, 320.0 mg (46%) ¹H NMR (500 MHz, Methanol-*d*₄) δ 8.38 (s, 1H), 7.96 (d, *J* = 8.4 Hz, 1H), 7.92 (d, *J* = 8.3 Hz, 1H), 4.25 (s, 2H). HRMS (ESI) *m/z*: calcd. for C₉H₆ClN₂O₄S [M-H]⁻: 272.9742; Found: 272.9734.

6-NS-02 was synthesized by a substitution reaction between **6-NS-01** and anhydrous 1-boc-piperazine. **6-NS-01** (200 mg, 0.73 mmol) and anhydrous 1-boc-piperazine (813.71 mg, 4.37 mmol) were placed into the 50 mL dry round bottom flask. And 30 mL anhydrous THF was added for reflux. After the **6-NS-01** was consumed completely by Thin-Layer Chromatography (TLC) analysis, the reaction was stopped. The intermediate product was purified by silica gel column chromatography and then treated with trifluoroacetic acid (TFA) to remove the boc-protecting group, yielding the final product **6-NS-02** as a white powder. Yield, 83.5 mg (35%). ¹H NMR (400 MHz, Deuterium Oxide) δ 7.85 (s, 1H), 7.51 (d, *J* = 8.3 Hz, 1H), 7.45 (d, *J* = 8.3 Hz, 1H), 3.20 (s, 2H), 3.06 (t, *J* = 4.5 Hz, 4H), 2.67 (t, *J* = 4.5 Hz, 4H). HRMS (ESI) *m/z*: calcd. for C₁₃H₁₅N₄O₄S [M-H]⁻: 323.0819; Found: 323.0810.

Synthesis of the compounds **PS-01** and **PS-02**

Under N₂ atmosphere, a mixture of **PS**² (200 mg, 0.26 mmol), 1,3-dibromopropane (158.2 mg, 0.78 mmol), and K₂CO₃ (105.3 mg, 0.78 mmol) was weighed and placed into a dry Schlenk flask. Then, anhydrous DMF (10 mL) was added by syringe. The mixture was stirred at 70 °C for overnight. When the **PS** completely disappeared in the reaction solution by TLC analysis, the reaction was terminated by adding 10 mL saturated ammonium chloride aqueous solution. Then, 20 mL ethyl acetate was added

and the mixture was washed with deionized water (50 mL×3) and the organic solution was further dried using anhydrous sodium sulfate. Lastly, the organic solution was removed under reduced pressure and the residue was further purified by silica gel column chromatography by using CH₂Cl₂/MeOH (v/v, 10/1) as the eluent. The product was obtained as black-red solid powders. **PS-Br**, Yield, 120.1 mg (52%). ¹H NMR (500 MHz, DMSO-*d*₆) δ 8.22 (d, *J* = 7.7 Hz, 1H), 8.01 (d, *J* = 16.0 Hz, 2H), 7.91 (t, *J* = 7.6 Hz, 1H), 7.81 (t, *J* = 7.7 Hz, 1H), 7.72 (d, *J* = 16.0 Hz, 2H), 7.62 (d, *J* = 7.2 Hz, 1H), 6.61 (s, 2H), 6.45 (s, 2H), 4.06 (t, *J* = 6.0 Hz, 2H), 3.22 (t, *J* = 6.9 Hz, 2H), 2.35 (s, 6H), 1.84 (t, *J* = 6.5 Hz, 2H). HRMS (ESI) *m/z*: calcd. for C₄₅H₂₆BrCl₂N₄O₇ [M-H]⁻: 883.0341; Found: 883.0367.

Under the N₂ atmosphere, a mixture of **PS-Br** (50 mg, 0.06 mmol), N-methyl piperazine (22.6 mg, 0.23 mmol), and K₂CO₃ (31.05 mg, 0.23 mmol) was suspended in 10 mL anhydrous DMF. The mixture was stirred at 70 °C for 12 h in the dark. When the **PS-Br** was completely consumed by TLC analysis, the reaction was terminated by adding 10 mL saturated ammonium chloride aqueous solution. Then, 20 mL ethyl acetate was added and the mixture was washed with deionized water (50 mL×3). The organic solution was collected and further dried using anhydrous sodium sulfate. Lastly, the organic solution was removed under reduced pressure and the residue was purified by silica gel column chromatography, CH₂Cl₂/MeOH (v/v, 8/1) as eluent. The product was obtained as black-red solid powders. **PS-01**, Yield, 25.0 mg (49%). **PS-01**, ¹H NMR (d-DMSO, 400 MHz, ppm): ¹H NMR (500 MHz, DMSO-*d*₆) δ 8.16 (d, *J* = 7.7 Hz, 1H), 7.97 (d, *J* = 16.0 Hz, 2H), 7.91 (t, *J* = 7.5 Hz, 1H), 7.81 (t, *J* = 7.8 Hz, 1H),

7.75 – 7.68 (m, 3H), 6.76 (s, 2H), 6.62 (s, 2H), 6.44 (s, 2H), 3.99 (t, $J = 6.0$ Hz, 2H), 2.66 (m, 10H), 2.35 (s, 6H), 2.04 (s, 3H), 1.40 (m, 2H). HRMS (ESI) m/z : calcd. for $C_{50}H_{37}Cl_2N_6O_7$ [M-H]⁻: 903.2106; Found: 903.2081.

The synthesis of **PS-02** followed the synthesis procedure of **PS-01** except that the N-methyl piperazine was replaced by legend **6-NS-02**. Yield, 18.0 mg (28%). **PS-02**, ¹H NMR (400 MHz, DMSO-*d*₆) δ 8.17 (d, $J = 8.2$ Hz, 2H), 8.05 (s, 1H), 7.99 (d, $J = 15.9$ Hz, 2H), 7.88 (t, $J = 7.3$ Hz, 2H), 7.83 – 7.75 (m, 3H), 7.71 (d, $J = 16.0$ Hz, 2H), 7.58 (d, $J = 7.5$ Hz, 1H), 7.49 (d, $J = 8.2$ Hz, 1H), 6.77 (s, 2H), 6.58 (s, 2H), 6.43 (s, 2H), 3.97 (t, $J = 6.2$ Hz, 2H), 3.08 (s, 2H), 2.39 (s, 4H), 2.32 (s, 6H), 2.20 (s, 4H), 1.98 (t, $J = 7.1$ Hz, 2H), 1.45 – 1.34 (m, 2H). ¹³C NMR (101 MHz, DMSO) δ 172.80, 169.39, 168.39, 165.88, 164.00, 162.12, 156.44, 154.81, 152.30, 146.81, 141.66, 133.55, 133.03, 131.15, 130.78, 130.62, 130.06, 129.38, 126.93, 123.39, 122.47, 118.50, 115.76, 115.62, 110.82, 109.92, 109.28, 106.03, 105.14, 64.18, 62.08, 55.27, 54.40, 53.21, 52.71, 25.66, 19.76. HRMS (ESI) m/z : calcd. for $C_{58}H_{41}Cl_2N_8O_{11}S$ [M-H]⁻: 1127.1998; Found: 1127.2000.

2.2 Steady-state Spectra Measurement.

The steady-state absorption and fluorescence spectra were recorded with a UV-Vis spectrometer named Cary 60 and a fluorometer named Cary Eclipse from Agilent Tech at room temperature, respectively. The relative fluorescence quantum yields were determined with Rhodamine B ($\Phi = 0.69$ in EtOH)³ as a standard and calculated using the following equation:

$$\Phi_{\text{sam}} = \Phi_{\text{std}} \times \frac{A_{\text{std}}}{A_{\text{sam}}} \times \frac{I_{\text{sam}}}{I_{\text{std}}} \times \frac{n_{\text{sam}}^2}{n_{\text{std}}^2}$$

where s_{am} and s_{std} respectively represent the unknown sample and the standard compound; Φ represents quantum yield; A represents the absorbance at the selected excitation wavelength; I represent the integrated area of the corrected emission spectrum; n represents the refractive index of the selected solvent.

2.3 Molecule docking calculation

The docking calculations of **PS-02/CAIX** were performed with AutoDock 4.2 using Lamarckian genetic algorithm method⁴. The structure of the CAIX was obtained from the RCSB Protein Data Bank (PDB code: 3IAI). The grid center coordinates were 65.930, 57.488, and 12.016, the grid size was $127 \times 127 \times 127$, the spacing was set to 0.375 Å, and the exhaustiveness was set to 50 iterations.

2.4 Nanosecond Time-resolved Transient Absorption Spectroscopy.

PS-01 or **PS-02** (10 μ M) in aqueous solutions was placed in a long-neck quartz cell with a closed rubber plug, and the solution was deoxygenated by argon bubble with a flow of 20 mL/min for at least 20 min. Nanosecond time-resolved transient absorption spectra were obtained using an LP920 laser flash photolysis spectrometer (Edinburgh Instruments, UK). The kinetic traces were recorded and the triplet state lifetime was obtained by fitting the decay curve using the lifetime meter software.

2.5. *In vitro* Reactive Oxygen Species (ROS) Detection Method

The amounts of ROS were detected by using the commercial ROS probe DCFH-DA. Firstly, the DCFH solution was prepared by hydrolyzing DCFH-DA in an alkaline solution. DCFH-DA solution (20 μ L, 10 mM) was added to NaOH solution (0.8 mL, 10 mM) and maintained at room temperature for 30 min in the dark. Then, the reactant

solution was transferred into PBS (50 mM, 4.18 mL) to obtain the DCFH solution. For ROS detection, DCFH solution (0.04 mM, 150 μ L) was added into **PS**, **PS-01**, or **PS-02** solution in quartz cells. The mixture was irradiated by white light LED (2 mW cm^{-2}) at different times. The fluorescence emission spectra of DCFH at 500-600 nm were recorded at various time to obtain the ROS generation rate of the photosensitizing process.

2.6 Cell Culture Conditions.

MDA-MB-31 cells were obtained from the Institute of Basic Sciences (IBMS) of the Chinese Academy of Medical Sciences (CAMS). The cell clones were cultured in DMEM medium supplemented with 10% fetal calf serum (FBS) and 1% streptomycin (0.1 mg mL^{-1}) at 37°C in 95% air with 5% CO_2 . 1×10^5 MDA-MB-31 cells were firstly plated onto 35 mm glass-bottom culture dishes and incubated for 24 h for specific fluorescence images.

2.7 Confocal Laser Scanning Microscopy Fluorescence Imaging of Intracellular ROS and cell membrane Colocalization.

MDA-MB-31 cells in the exponential phase of growth were grown on 35 mm glass-bottom culture dishes for 24-36 h to reach about 80% confluency. The cells were washed three times with PBS and then incubated with 1 mL DMEM containing **PS NPs**, **PS-01 NPs**, or **PS-02 NPs** (5 μ M) in an atmosphere of 95% air with 5% CO_2 for 6 h at 37°C. The cells were further stained by DiO (10 μ M), DHR123 (10 μ M) or DCF-DA (1 μ M). The medium was replaced with a fresh one. Cells were then visualized with confocal laser scanning microscopy. The excitation wavelength for **PS NPs**, **PS-01 NPs**

or **PS-02 NPs** was 559 nm, while the excitation wavelength for DND-26 or DHR123 or DCF-DA was 488 nm. And the detection wavelength was from 570 to 670 nm for **PS NPs, PS-01 NPs** or **PS-02 NPs**, 515 to 555 nm for DND-26 or DHR123 or DCF-DA. To avoid color crosstalk between two fluorescence channels, sequence scanning mode was used during data collection.

2.8 Fluorescence Imaging of Live and Dead Cells.

4T1 cells were plated onto 35 mm glass-bottom culture dishes for 24 h and incubated with **PS NPs, PS-01 NPs, or PS-02 NPs** (5 μ M) for 6 h. After irradiating for 15 min with white light LED (20 mW/cm²), cells were stained with Calcein (AM)/propidium iodide (PI) apoptosis detection kit according to the manufacturer's instructions. The cell apoptosis was visualized by CLSM imaging. AM: excitation wavelength 488 nm and detection wavelength 515-555 nm; PI: excitation wavelength 559 nm and detection wavelength 590-630 nm.

2.9 MTT Assay.

4T1 cells were seeded on 96 well plates (3×10^3 cells per well) and cultured for 24 h. **PS NPs, PS-01 NPs, or PS-02 NPs** with different concentrations were added and co-incubated for 6 h, respectively. Then the cells were washed three times with PBS and irradiated with white light LED (20 mW/cm²) for 15 min. After irradiation, the cells were incubated for another 24 h. The relative cell viability was evaluated by stander MTT assay.

2.10 PDT Evaluation *in vivo*

All the animal experiments involved in this study were conducted in accordance with the Guide for the Care and Use of Laboratory Animals published by the US National Institutes of Health, and approved by the local research ethics review board of the Animal Ethics Committee of Dalian University of Technology. Female BALB/c mice, 6-7 weeks old, originally purchased from the SPF Experimental Animal Center of Dalian Medical University, were used to establish a breast cancer mouse model. Briefly, 1×10^6 4T1 cells were injected subcutaneously into the selected positions to establish the breast tumor model of BALB/c mice. Tumors were allowed to grow to about 200 mm³ in volume before being used for *in vivo* imaging and phototherapy. The *in vivo* biosafety assay was performed by mice body weight and H&E slice histological analysis. After the 14th day of treatment, all mice were sacrificed and the tumor tissues and the main organs including heart, liver, spleen, lung, and kidneys were harvested for histological analysis by means of hematoxylin and eosin (H&E) staining.

3. Figures and tables

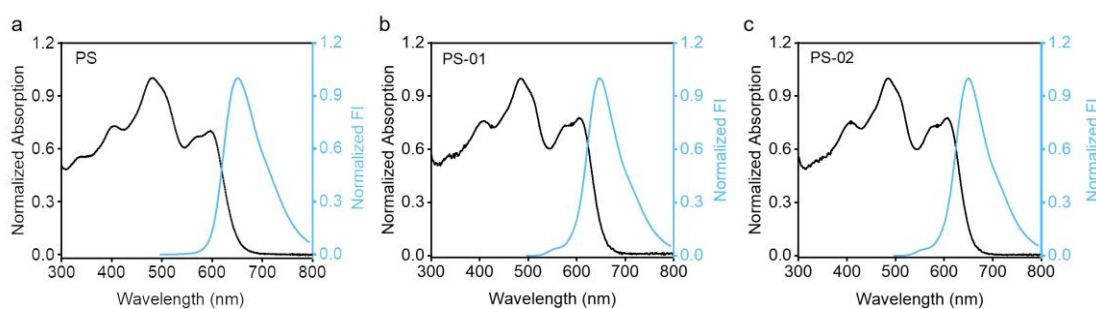


Figure S1. Normalized UV-Vis absorption and fluorescence emission spectra of **PS** (a), **PS-01** (b), and **PS-02** (c) (10 μ M) in DMF (Excitation wavelength λ_{ex} =480 nm).

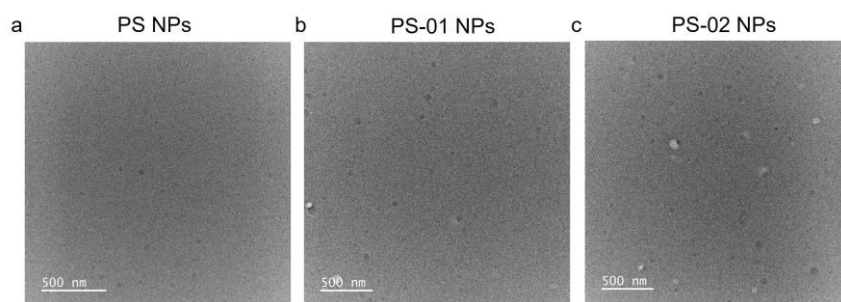


Figure S2. TEM photograph of **PS NPs** (a), **PS-01 NPs** (b) and **PS-02 NPs** (c).

Table S1. Relative fluorescence quantum yield of **PS**, **PS-01**, **PS-02** and **PS-02/CAIX** in aqueous solution

compounds	Φ^a_{Fl}
PS	100%
PS-01	43%
PS-02	93%
PS-02/CAIX	28%

^a To compare simply and clearly, the fluorescence quantum efficiency of **PS** in an aqueous solution was defined as 100%.

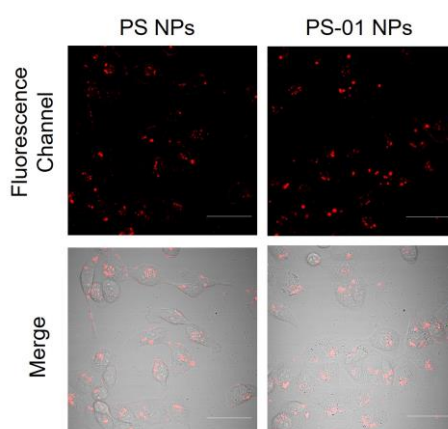


Figure S3. The CLSM imaging of MDA-MB-231 cells stained by **PS NPs** or **PS-01 NPs**, respectively, excitation light source 559 nm, detection channel 620±20 nm, scale bar = 50 μm.

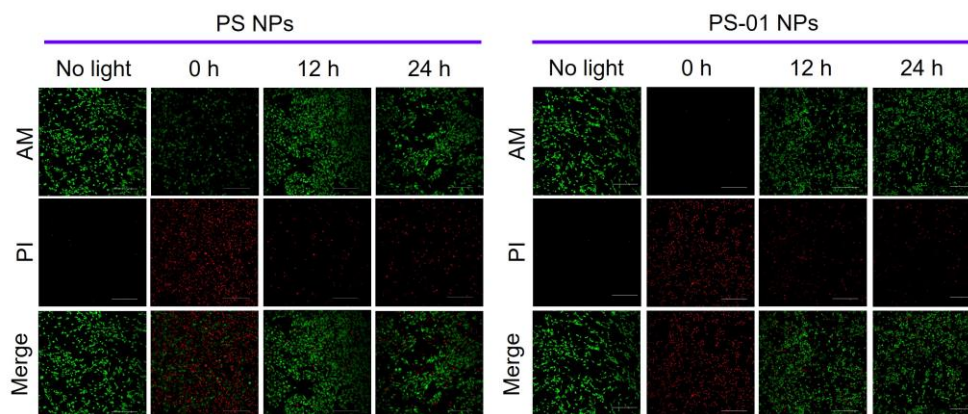


Figure S4. CLSM image of live and dead cells treated with **PS NPs** and **PS-01 NPs** (5 μM) under light treatment by calcein AM (2 μM)/propidium iodide (PI) (4 μM) staining. After the cells once stained by **PS NPs** or **PS-01 NPs**, the same light treatment was conducted at 0 h, 12 h, and 24 h, respectively. (Calcein AM: excitation light source 488 nm, detection channel wavelength = 530 ± 20 nm; PI: excitation light source 559 nm, detection channel wavelength = 650 ± 50 nm), scale bar = 300 μm.

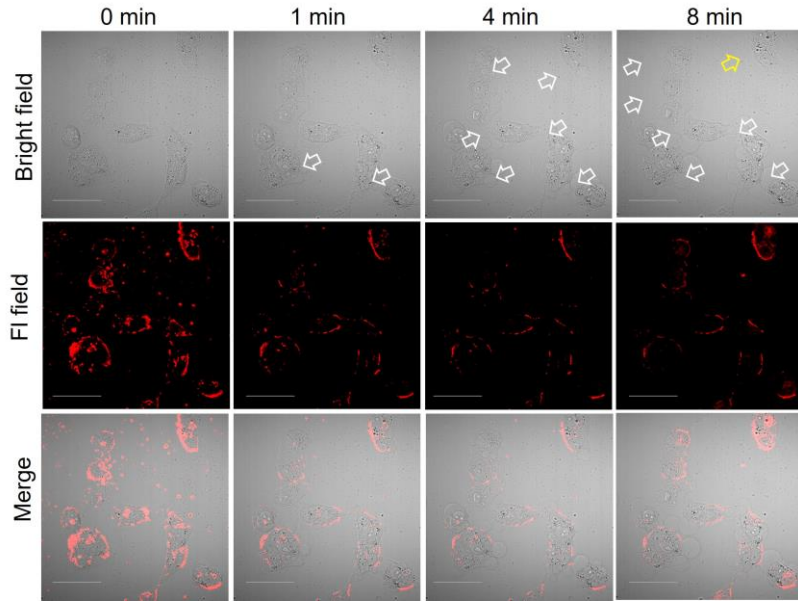


Figure S5. CLSM imaging of MDA-MB-231 cells treated by **PS-02 NPs** ($5 \mu\text{M}$) at different times after light irradiation. Scale bars: 50 mm (LED 630 nm, 20 mW cm^{-2}), The white arrow pointed to the bubbles around the cell membrane, and the yellow arrow pointed to the ruptured cell.

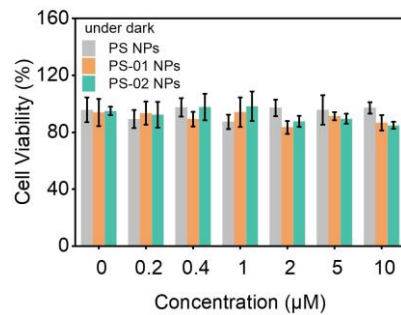


Figure S6. Relative viabilities of MDA-MB-231 cells treated with different concentrations of **PS NPs**, **PS-01 NPs**, and **PS-02 NPs** under dark treatment.

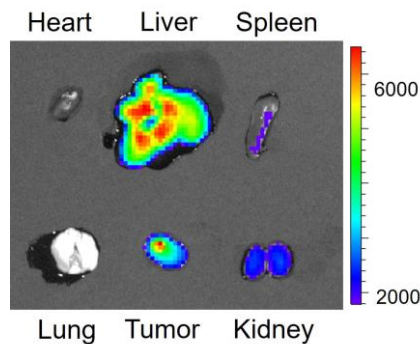


Figure S7. *Ex vivo* fluorescence imaging of major organs including heart, liver, spleen, lung, and kidney, as well as tumor at 36 h after intravenous injection of **PS-02 NPs**.

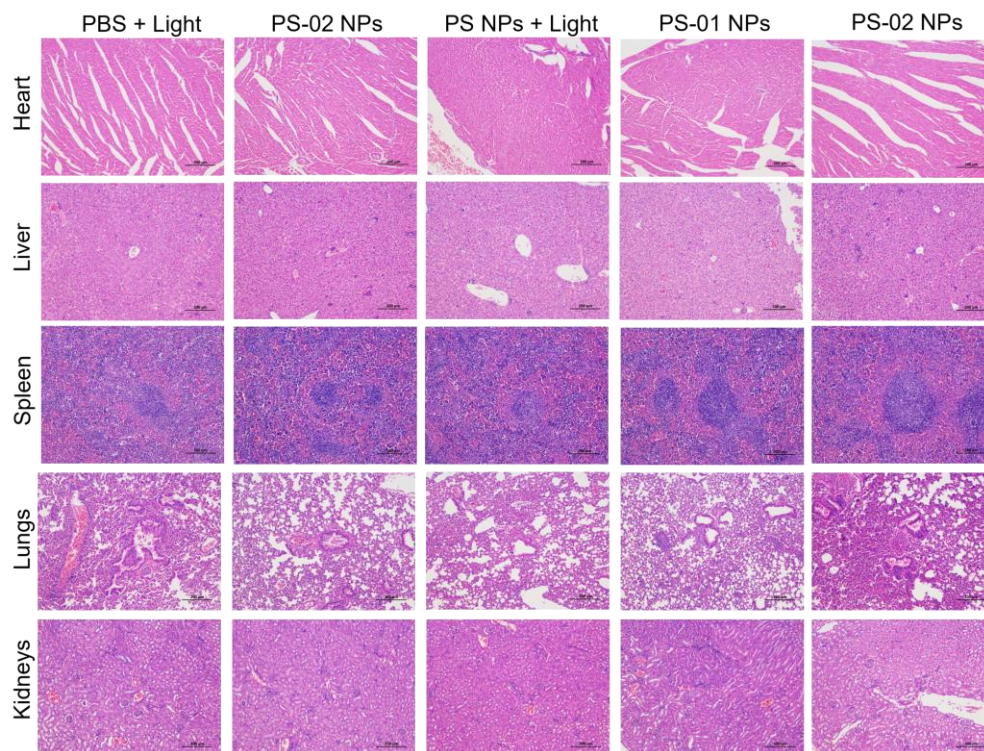


Figure S8. *In vivo* biosafety assay of H&E staining the major organs of mice from different treatment groups on the 14th day after treatment. Scale bar = 200 μm .

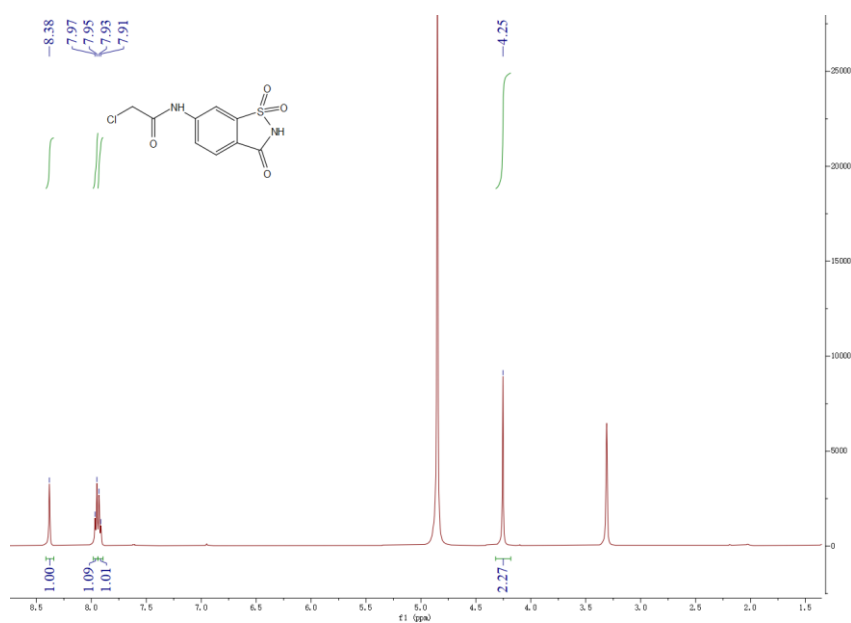


Figure S9. ^1H NMR spectra of **6-NS-01** (in methanol- d_4).

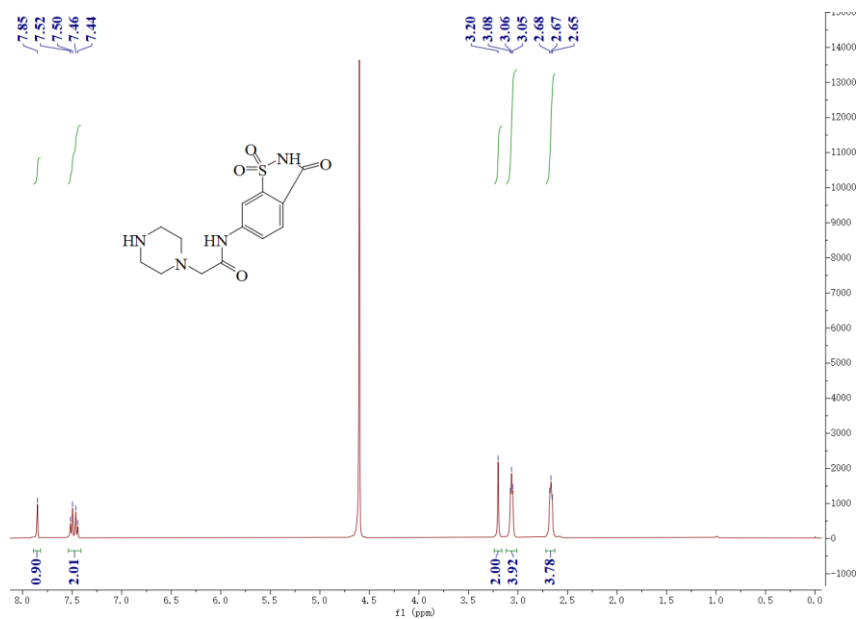


Figure S10. ^1H NMR spectra of 6-NS-02 (in Deuterium Oxide).

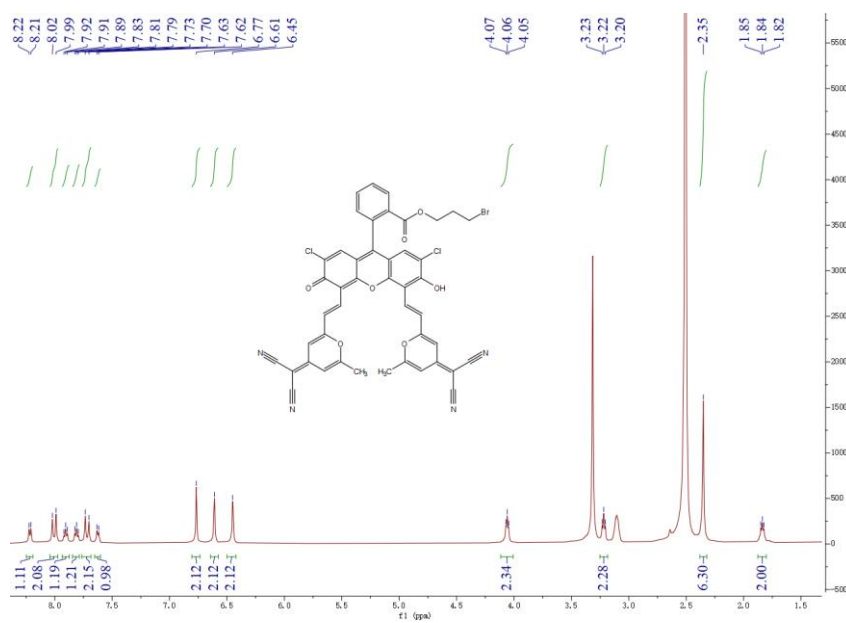


Figure S11. ^1H NMR spectra of PS-Br (in DMSO- d_6).

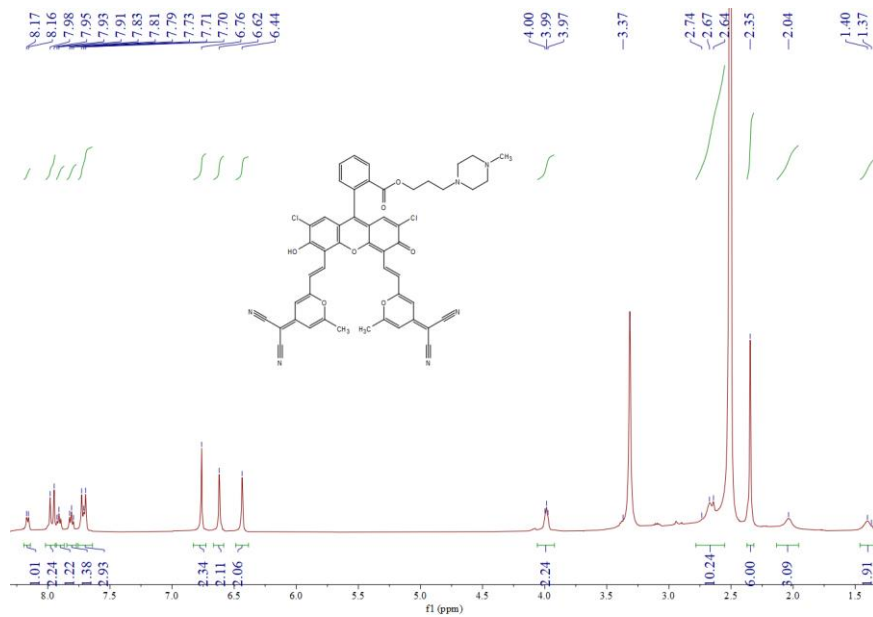


Figure S12. ¹H NMR spectra of PS-01 (in DMSO-d₆).

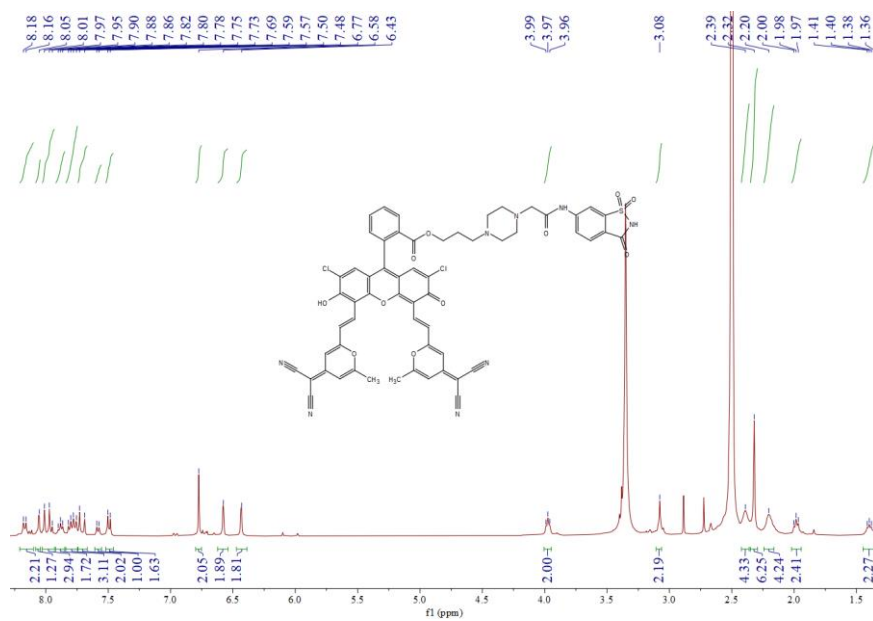


Figure S13. ¹H NMR spectra of PS-02 (in DMSO-d₆).

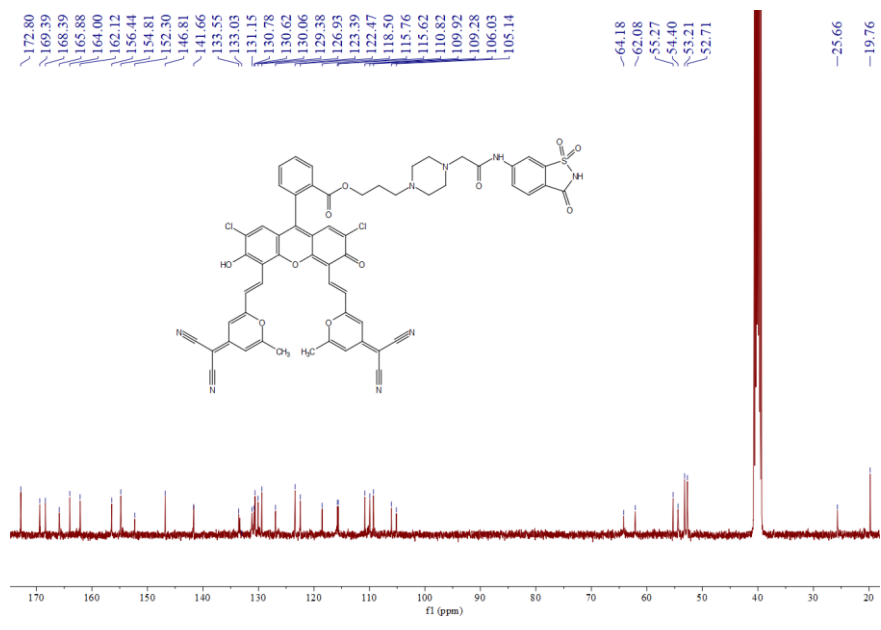


Figure S14. ¹³C NMR spectra of PS-02 (in DMSO-d6).

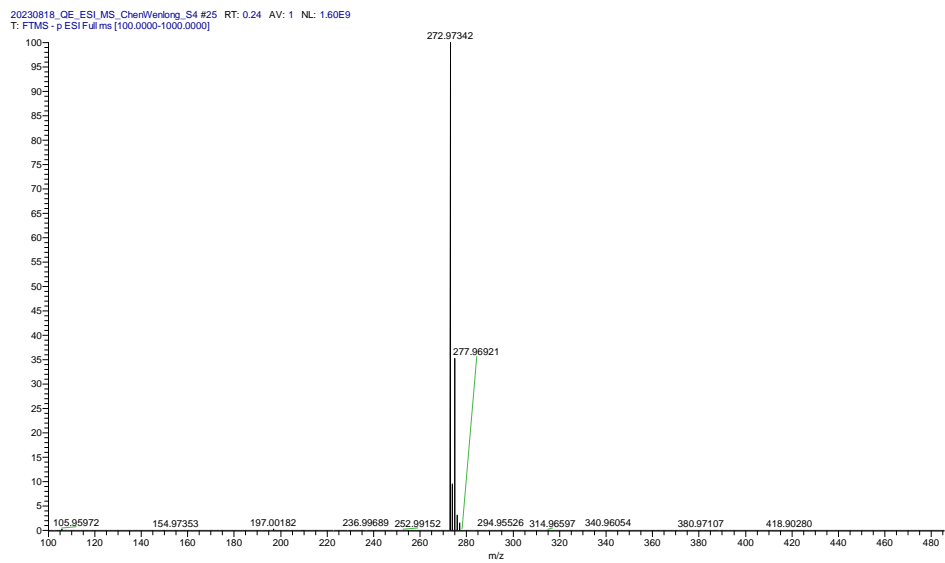


Figure S15. HRMS spectra of 6-NS-01

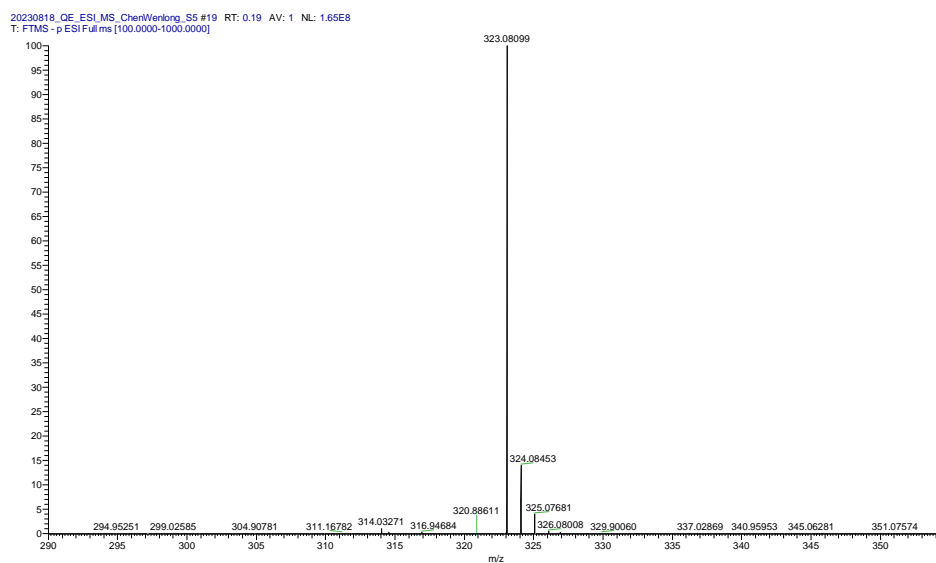


Figure S16. HRMS spectra of **6-NS-02**

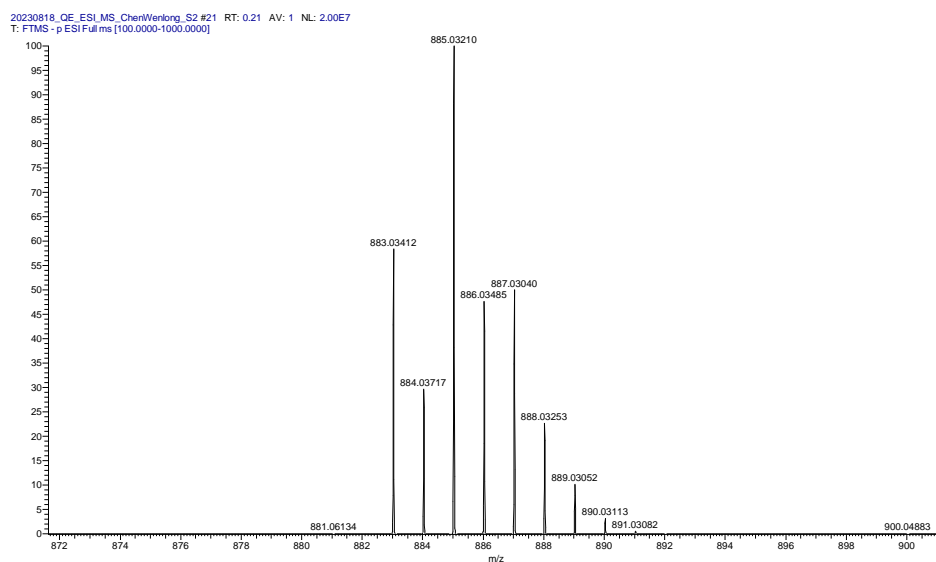


Figure S17. HRMS spectra of **PS-Br**

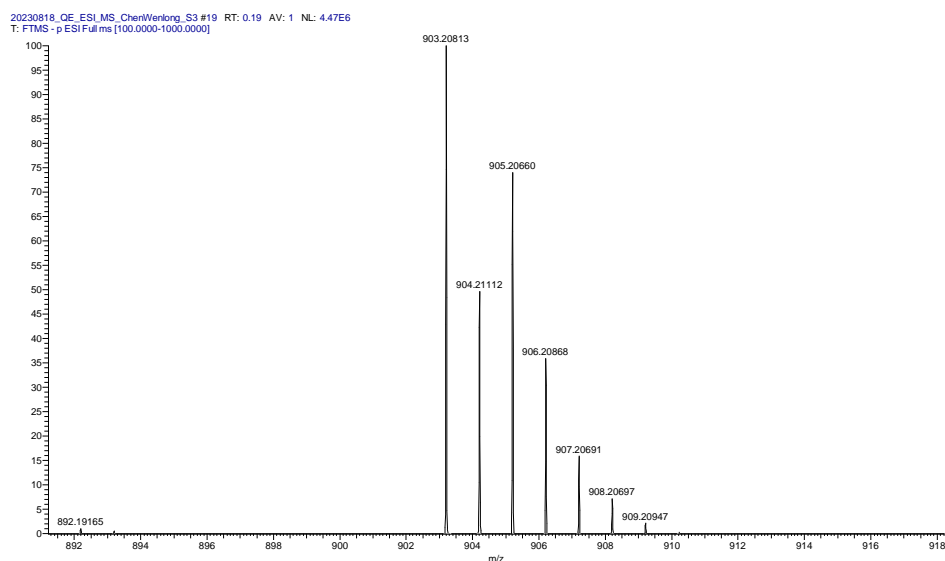


Figure S18. HRMS spectra of PS-01

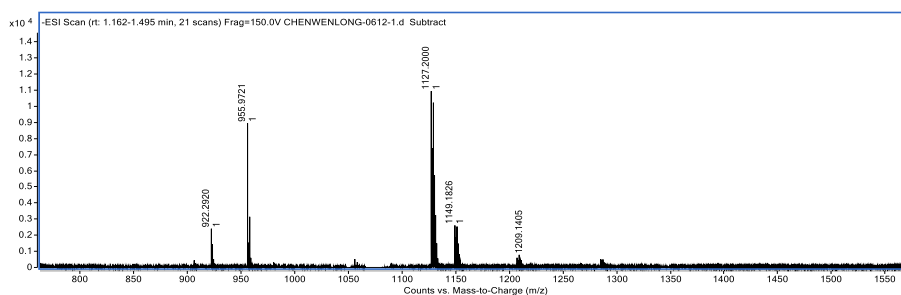


Figure S19. HRMS spectra of PS-02

References:

1. Zhang, S. Y.; Yang, C. M.; Lu, W. Q.; Huang, J.; Zhu, W. P.; Li, H. L.; Xu, Y. F.; Qian, X. H., A highly selective space-folded photo-induced electron transfer fluorescent probe for carbonic anhydrase isozymes IX and its applications for biological imaging. *Chem. Commun.* **2011**, 47 (29), 8301-8303.

2. Xiong, X. Q.; Song, F. L.; Sun, S. G.; Fan, J. L.; Peng, X. J., Red-Emissive Fluorescein Derivatives and Detection of Bovine Serum Albumin. *Asian J. Org. Chem.* **2013**, *2* (2), 145-149.

3. Kubin, R. F.; Fletcher, A. N., Fluorescence quantum yields of some rhodamine dyes. *J. Lumin.* **1982**, *27* (4), 455-462.

4. M. J. Frisch, G. W. Trucks, H. B. Schlegel, G. E. Scuseria, M. A. Robb, J. R. Cheeseman, G. Scalmani, V. Barone, B. Mennucci, G. A. Petersson, H. Nakatsuji, M. Caricato, X. Li, H. P. Hratchian, A. F. Izmaylov, J. Bloino, G. Zheng, J. L. Sonnenberg, M. Hada, M. Ehara, K. Toyota, R. Fukuda, J. Hasegawa, M. Ishida, T. Nakajima, Y. Honda, O. Kitao, H. Nakai, T. Vreven, J. A. Montgomery, J. J. Peralta, F. Ogliaro, M. Bearpark, J. J. Heyd, E. Brothers, K. N. Kudin, V. N. Staroverov, R. Kobayashi, J. Normand, K. Raghavachari, A. Rendell, J. C. Burant, S. S. Iyengar, J. Tomasi, M. Cossi, N. Rega, J. M. Millam, M. Klene, J. E. Knox, J. B. Cross, V. Bakken, C. Adamo, J. Jaramillo, R. Gomperts, R. E. Stratmann, O. Yazyev, A. J. Austin, R. Cammi, C. Pomelli, J. W. Ochterski, R. L. Martin, K. Morokuma, V. G. Zakrzewski, G. A. Voth, P. Salvador, J. J. Dannenberg, S. Dapprich, A. D. Daniels, Ö. Farkas, J. B. Foresman, J. V. Ortiz, J. F. D. Cioslowski, Gaussian, Inc., Wallingford CT, 2016.